System reliability analysis of downstream spillways based on collapse of upstream spillways

Won Choi[1], Jeongbae Jeon[2], Jinseon Park[2], JeongJae Lee[3], Seongsoo Yoon[2*]

(1. *Department of Rural Systems Engineering, College of Agriculture and Life Sciences, Seoul National University, Seoul 151-921, South Korea*; 2. *Department of Agricultural and Rural Engineering, College of Agriculture, Life and Environments Sciences, Chungbuk National University, Chungbuk 362-763, South Korea*; 3. *Department of Rural Systems Engineering, Research Institute of Agriculture and Life Sciences, College of Agriculture and Life Sciences, Seoul National University, Seoul 151-921, South Korea*)

Abstract: Some agricultural reservoirs in South Korea are vulnerable to situations in which they are unable to function as reservoirs because of essential safety issues. This is because 70% of existing agricultural reservoirs were originally constructed more than 50 years ago; most of these reservoirs have not been maintained or managed since their initial construction. In the worst cases, reservoirs are connected to one another by short distances and/or the sizes of upstream reservoirs are larger than the sizes of downstream reservoirs. Individual components of the reservoirs, such as their embankments, spillways, and water intake facilities, have been considered in order to understand the main factors associated with potential reservoir failure. Accordingly, this study aims to estimate the probability of failure in downstream spillways upon the collapse of upstream spillways (for reservoirs connected in series). A simple equation to calculate the rise in the water level in downstream spillways, which is caused by the collapse of upstream spillways, was proposed. This equation was based on the discharge equation of an overflowing rectangular weir and the scaling law for continuous flow. To verify the proposed simple equation, the water level increments were compared with the simulated results of the commercial software FLOW-3D, which is an accurate computational fluid dynamics (CFD) program that is used for tracking free-surface flows. The values predicted through the simple formula were close to the simulated data (within a maximum prediction error of 5%). The values were updated to reflect the effects of hydraulic pressures on the walls of downstream spillways, thereby allowing the failure probabilities (due to overturning, sliding, and settlement) of the downstream spillways to be computed. This study found that the failure probabilities of independent components in reservoirs are significantly different from the systematic failure values observed in sequential modes.

Keywords: failure probability, collapse, spillway, discharge, scaling law, FLOW-3D

DOI: 10.3965/j.ijabe.20150804.1824

Citation: Choi W, Jeon J, Park J, Lee J, Yoon S. System reliability analysis of downstream spillways based on collapse of upstream spillways. Int J Agric & Biol Eng, 2015; 8(4): 140－150.

1 Introduction

The total number of reservoirs in South Korea is around 18 000, but the Korea Rural Community Corporation (KRC) maintains or manages only about 3 000 reservoirs. The other 15 000 reservoirs, which are under the management of local authorities are without adequate supervision, due to shortages in local budgets

Received date: 2015-03-30 **Accepted date:** 2015-07-24

Biographies: Won Choi, PhD, Postdoctoral researcher, Research interests: agricultural engineering applications using multiphysics models and especially agricultural structure engineering, Email: fembemwonchoi@gmail.com. **Jeongbae Jeon,** PhD Candidate, Researcher, Research interests: agricultural structural systems, Email: maxnight703@nate.com. **Jinseon Park,** PhD, Postdoctoral researcher, Research interests: agricultural structural systems, Email: kohibito99@lycos.co.kr. **JeongJae Lee,** PhD, Professor, Research interests: structural and systems engineering, Email: ljj@snu.ac.kr.

***Corresponding author: Seongsoo Yoon,** PhD, Professor, Research interests: agricultural architecture, structural design and automation system. Department of Agricultural and Rural Engineering, College of Agriculture, Life and Environments Sciences, Chungbuk National University, 1 Chungdae-ro, Seowon-Gu, Cheongju, Chungbuk 362-763, South Korea. Tel: +82-43-261- 2575, Email: yss@cbnu.ac.kr.

and human resources. Seventy percent of these reservoirs were constructed more than 50 years ago. Furthermore, sixty percent of the annual precipitation in South Korea falls in the months of August, September, and October. For reference, the monthly maximum precipitations in Japan (Osaka, June, 206.4 mm), Canada (Vancouver, December, 178.4 mm), USA (Atlanta, March, 146.6 mm), and China (Shanghai, September, 155.5 mm), are much lower than the maximum average monthly precipitation in South Korea (Seoul, August, 348 mm); this increased precipitation is due to typhoons in the western part of the North Pacific Ocean. For example, typhoon Rusa damaged 52.4% of Korea's sluiceways and spillways (including 26.7%, 12.4%, and 8.6% of the embankments, siltations, and retaining walls of South Korean reservoirs, respectively) in 2002. The precision safety diagnosis report from the KRC in South Korea asserts that the individual safety factors of the components of old reservoirs have decreased. Moreover, many reservoirs are connected in series and are parallel to one another within short distances.

Recently, the collapse of spillways has been reported frequently in South Korea. The retaining walls of the spillway of the Josan reservoir (located in Gochang City, Jellabuk-do) collapsed in July of 2013. The reservoir, which was constructed in 1956, consists of an embankment length of 231.7 m, a height of 20.56 m, and a volume of 55 680 m^3. According to reports from the weather station near the province, the rainfall was greater than 300 mm on the day prior to the collapse. Approximately 20 m of the retaining walls and additional portions of the embankment were lost due to the heavy rain; as a result, the KRC evacuated 2000 residents from the province.

In August of 2014, the entire spillway of the Goeyeon reservoir (located in Yeongcheon City, Gyeongsangbuk-do) and 30 m of the retaining walls collapsed due to sudden, heavy rains (227.8 mm over a period of five days). This reservoir, which was constructed in 1945, has an embankment length of 160 m, a height of 5.5 m, and a total volume of 61 000 m^3. This accident caused a state of emergency and affected 500 people in three downstream villages. More than 20 houses and approximately 100 000 m^2 of farmlands, including roads, guardrails, and facilities, were flooded.

A representative example of catastrophic reservoir failure occurred in August of 1975 in Zhumadian, Henan, China[20]. The typhoon Nina dumped 1 631 mm of precipitation over a period of five days, which was well beyond the planned design capacities of the Banqiao and Shimantan reservoirs on the Ru and Hong Rivers, respectively. The two large reservoirs collapsed, causing 62 smaller downstream reservoirs to fail via overtopping. The breaching of these reservoirs led to a water-inundated area of 12 000 km^2, the death of 171 000 people, and an economic loss of more than 10 billion RMB. To avoid these types of safety issues, it is necessary to understand how engineers prioritize repairs and how the collapse of upstream reservoirs affects downstream reservoirs.

Therefore, multiple failure modes should be considered for the reliable analysis of relationships between reservoirs. The system failure modes can be divided into three types: parallel systems, serial systems, and a combination of serial and parallel subsystems. A parallel system collapses when all elements comprising the parallel system are destroyed, whereas a serial system is destroyed when any one of the elements reaches its limit state. One concern in this study is how the collapse of an upstream reservoir spillway influences the failure probability of downstream reservoirs (i.e., the upstream and downstream reservoirs being an example of a serial system); the possibility for serial systems to be involved in dangerous situations is generally higher.

To the best of our knowledge, few publications have intensively studied the failure probabilities of systems by defining the relationships between reservoir components. Accordingly, our research conducts calculations concerning the failure probability of downstream spillways from the perspective of system dynamics. Our worst-case scenario assumes that the collapse of an upstream spillway could cause a rise in the water level of a downstream spillway. A simple equation, based on the discharge equation of an overflowing weir and the scaling law, is proposed as a method to estimate the rise of the water level of a downstream spillway without

simulating a transient 3-D computational fluid dynamics (CFDs) model. This calculated value is used to compute the failure probability of the downstream spillway.

2 Targeted area and random variables

2.1 Targeted area

To investigate the failure probability of the spillway of a downstream reservoir following the collapse of the spillway of an upstream reservoir, two cases of reservoirs directly connected in series were selected from the 24 reservoirs located in the Sheokwha River area in Cheongju City, Chungcheongbuk-do, South Korea. The two pairs of upstream and downstream reservoirs are: 1) Dabaemi and Darakmal and 2) Anmal and Naesuinpyeong, respectively, as shown in Figure 1.

The Rural Agricultural Water Resource Information System (RAWRIS) of the KRC in South Korea has provided basic data about the irrigation facilities associated with rural waterways. Information about the targeted reservoirs is shown in Table 1.

Because rehabilitation projects and upgrades had been conducted several times for each of the four reservoirs, which were constructed prior to 1945, it is difficult to acquire the original field data. The geometric shapes of the spillways have been discerned using field instrumentation, as shown in Figure 2.

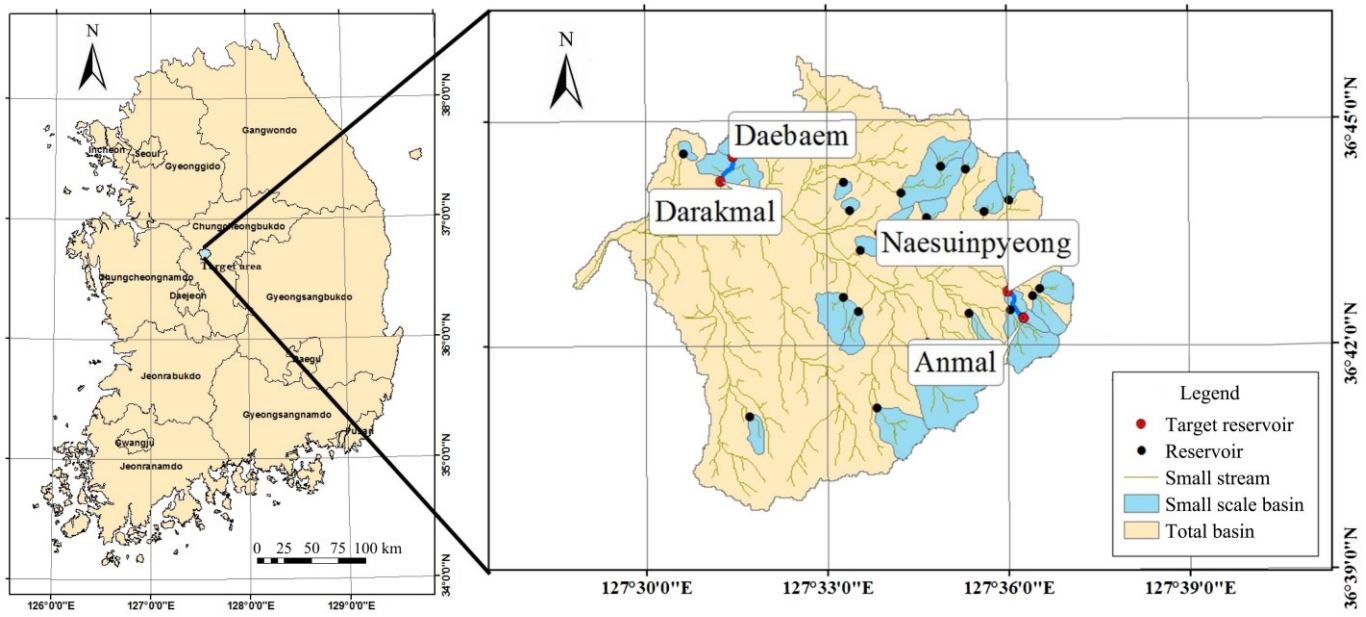

Figure 1 Geometric topography of reservoirs

Table 1 Information about the targeted reservoirs

Reservoir	Location		Watershed area/ha	Beneficial area/ha	Spillway type	Year of completion
	Latitude/°N	Longitude/°E				
Daebaemi	36.74475	127.52531	34	5	Measuring channel	Prior to 1945
Darakmal	36.73928	127.53013	71	4	Measuring channel	Prior to 1945
Anmal	36.70903	127.60521	18	6	Measuring channel	Prior to 1945
Naesuinpyeong	36.71424	127.60047	32	6	Measuring channel	Prior to 1945

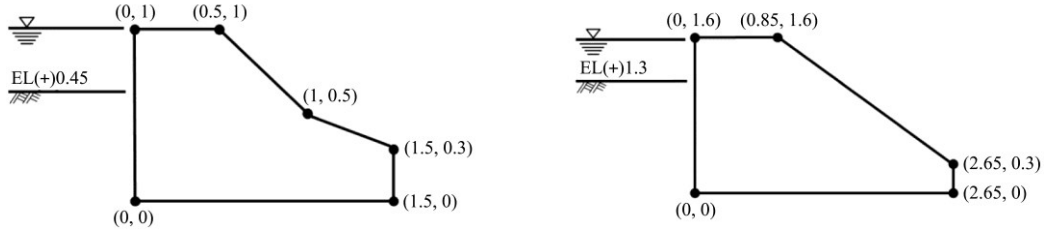

a. Darakmal b. Naesuinpyeong

Figure 2 Geometric shapes of the spillways of the reservoirs

2.2 Random variables

All parameters required for this research should be random variables due to the fact that these characteristics cannot be expressed as a single value. These random variables can be classified into two major parameters that are related to either concrete or soil, according to the material characteristics. Because concrete is a combined material composed of cement, sand, gravel, and water, the unit weight of concrete varies depending on variations in the field conditions such as the composition, mixing, casting, curing, and so on. The Korea Occupational Safety and Health Agency (KOSHA) reported a value of 24 kN/m^3 as the typical unit weight of reinforced concrete. Previous studies[4,6] have shown that the coefficient of variation of the unit weight of concrete ranges from 0.02 to 0.05. In this study, 0.02 was selected as the coefficient of variation by accounting for the characteristics of materials in South Korea. The uncertainty related to soil is relatively greater than the uncertainties related to other structural materials because the material properties of soil are highly variable depending on time and space. Although the strength of soil can be determined experimentally, the results may be inconsistent. This inconsistency is due to material characteristics such as inhomogeneity, sample disturbance, a limited number of samples, the experimental method that is used, the level of proficiency of the researcher, and so on. The soil parameters used to calculate the failure probability are obtained from the statistical data of the precision safety diagnosis report[13] of the KRC in South Korea and the Emergency Action Plan (EAP) report[12] in the USA, as shown in Table 2.

Table 2 Soil parameters for probability analysis

Variables	Units	Average	Variance	Probability distribution
Water unit weight (γ_t)	kN/m^3	9.800	0.000	-
Saturated soil unit weight (γ_{sat})	kN/m^3	9.422	0.260	Normal distribution
Soil friction angle (φ_1)	°	28.445	0.252	Normal distribution
Soil friction angle (φ_2)	°	19.059	0.386	Normal distribution
Soil cohesion coefficient (c_1)	kN/m^3	18.846	0.607	Normal distribution
Soil cohesion coefficient (c_2)	kN/m^3	32.869	0.715	Normal distribution

Note: Superscripts 1 and 2 indicate fill and ground materials, respectively.

3 Calculation of water level

3.1 Basic assumptions

In the agricultural areas of South Korea, the slopes of natural streams range from 0.1% to 1.0%. 70% and 82% of small streams have slopes under 0.3% and total lengths below 3 km, respectively. Thus, the following properties were assumed based upon the topographical characteristics of South Korea:

1) The ideal shape of the water storage area of a reservoir is circular.

2) The slope of a natural main stream inflowing into a reservoir is low in comparison to the average slope of a stream connecting an upstream reservoir to a downstream reservoir.

3) The surface roughness of streams is extremely large because streambeds are composed of gravel and rocks.

4) The velocity of a stream inflowing into a reservoir is close to zero because its velocity is governed by a hydraulic phenomenon (the environmental characteristics at the outlet of the main stream) similar to the sudden expansion from a small channel to an infinite channel.

5) There are many opportunities to reduce the velocity of a stream during its flow because the total length of a stream is much larger than the width of the stream.

6) The peak discharge rates associated with the intensities of rainfall in the basin areas surrounding the targeted reservoirs are neglected because the discharge rates are much smaller than the values induced by the breaking of spillways.

Therefore, based on the assumptions above, the hydraulic velocity head and negative wave were not considered in this study.

3.2 Simple method

Most of the weirs among the agricultural reservoirs in South Korea are a type of broad-crested open rectangular weir. The discharge rate (Q) of water flowing over this type of weir can be calculated as follows:

$$Q = CLH^{1.5} \tag{1}$$

where, Q is the water flow rate of the weir; C is the coefficient of the weir; L is the length of the weir, and H is the head of the weir.

Because the flow of water through the whole domain is continuous and the outlet velocity of the intermediate stream that connects upstream and downstream reservoirs is theoretically zero, the geometric conditions of the

intermediate stream cannot cause the head to increase over the downstream weir. If all variables are equivalent, the head over the downstream weir will increase only if the water area of the upstream reservoir increases. Thus, a simple equation using the discharge rate and scaling law is established as follows:

$$1=\left(\frac{H_U^{1.5}}{H_D^{1.5}}\right)\left(\frac{L_U}{L_D}\right)\left(\frac{A_U}{A_D}\right) \quad (2)$$

where, U and D represent the variables related to the upstream and downstream reservoirs, respectively, and A is the water area of the reservoir.

Equation (2) can be algebraically rearranged into the following:

$$H_D=\left(H_U^{1.5}\left(\frac{L_U}{L_D}\right)\left(\frac{A_U}{A_D}\right)\right)^{\frac{1}{1.5}} \quad (3)$$

Therefore, the water head over the weir of the downstream reservoir can be estimated from Equation (3).

4 Numerical simulation

This study executed a transient three-dimensional computational flow dynamics simulation using the commercial software FLOW-3D to prove Equation (3).

4.1 FLOW-3D

FLOW-3D was developed to solve the dynamics of free surface flow based on the finite volume method (FVM), which is a numerical method used to solve the partial difference equation (PDE) expressed in the form of the mass conservation equation based on the divergence theorem[7]. The computational domain can be subdivided into hexahedral cells of different sizes in a Cartesian coordinate system. All variables are located at the centers of each cell, whereas velocities and fractional areas are located on the centers of cell faces normal to their coordinate system. The program calculates averaged values of each cell, and discrete times are updated by a staggered grid technique[19]. The method applies two representative techniques: the volume of fluid (VOF) and the structured fractional area-volume obstacle representation (FAVOR). The VOF is a special advection method used to define the sharp interface between water and air in one cell without using a fine mesh[15]. The VOF is an Eulerian fixed-grid technique that can compute the free water surface. The FAVOR technique can fully generate structured boundaries throughout the whole flow domain using the grid porosity, of which the value is zero or one (depending on the percentage of the solid volume)[8]. The structured FAVOR method, which eliminates flow losses that may result from using a Cartesian grid system, was implemented into the software to obtain accurate geometric representations of complex geometries in the computational domain based on regular volume cells[9]. Over the past few decades, many studies have applied the FLOW-3D software to the numerical simulation of fluid dynamics in order to understand spillway effects and dam breaks[5,10,11,17,18].

4.2 Governing equations

4.2.1 Time-averaged flow equations

We assumed one-phase fluid flow at an incompressible state. In the absence of diffusion, with sources and sinks of the fluid, the continuum and momentum equations governing transient three-dimensional flow are defined as follows:

$$\text{Continuity: } \frac{\partial}{\partial x_i}(u_i A_i)=0 \quad (4)$$

$$\text{Momentum: } \frac{\partial u_i}{\partial t}+\frac{1}{V_F}\left(u_j A_j \frac{\partial u_i}{\partial x_j}\right)=-\frac{1}{\rho}\frac{\partial P}{\partial x_i}+g_i+f_i \quad (5)$$

where, u is the velocity required to go through the face of a cell; A is the face area of the cell; t is the flowing time; V_F is the fluid volume fraction of the cell; ρ is the density of the fluid; P is the pressure of the cell; g is the body acceleration of the cell; f is the viscous acceleration of the cell, and x_i is the axis in the subscript direction (i) of the three-dimensional Cartesian coordinate system.

The viscous accelerations related to the dynamic viscosity (μ) are expressed below.

$$\text{Viscous acceleration: } \rho V_F f_i=wsx_i-\frac{\partial}{\partial x_j}(A_j\tau_{ij}) \quad (6)$$

where, wsx is the wall shear stress; τ is the shear stress, $\tau_{ii}=2\mu\left\{\frac{\partial u_i}{\partial x_i}-\frac{1}{3}\left(\frac{\partial u_j}{\partial x_j}\right)\right\}$, and $\tau_{ij}=-\mu\left\{\frac{\partial u_j}{\partial x_i}+\frac{\partial u_i}{\partial x_j}\right\}$, $(i,j)=(1,2),\ (1,3),\ (2,3)$.

In this model, the wall shear stresses are set to be zero

by assuming that the tangential velocities on the walls are zero.

The VOF function (F), which is used to define the ratio of fluid to the unit volume, is applied to track the free surface of the fluid. The VOF transportation equation is defined as follows:

$$\text{VOF: } \frac{\partial F}{\partial t}+\frac{1}{V_F}\left\{\frac{\partial}{\partial x}\left(FA_i u_i\right)\right\}=0 \tag{7}$$

4.2.2 Renormalized group (RNG) turbulent model

The RNG turbulent model was utilized to calculate the turbulent flow with respect to time and space. The transport equations related to the turbulent kinetic energy (k) and turbulent kinetic energy dissipation rate (ε) are shown below.

$$\frac{\partial k}{\partial t}+\frac{1}{V_F}\left\{u_i A_i \frac{\partial k}{\partial x_i}\right\}=P+Diff_k-\varepsilon \tag{8}$$

$$\frac{\partial \varepsilon}{\partial t}+\frac{1}{V_F}\left\{u_i A_i \frac{\partial \varepsilon}{\partial x_i}\right\}=C_1\frac{\varepsilon}{k}P+Diff_\varepsilon-C_2\frac{\varepsilon^2}{k} \tag{9}$$

where, P is the turbulent kinetic energy production; $Diff_k$ is the diffusion of k, $Diff_\varepsilon$ is the diffusion of ε, and C_1 and C_2 are dimensionless user-adjustable parameters.

In this RNG turbulent model, values of 1.42 and 1.68 were used for C_1 and C_2, respectively.

4.2.3 Kinematic turbulent viscosity

In all turbulent transport equations, the kinematic turbulent viscosities are computed as follows:

$$\nu=CNU\frac{k^2}{\varepsilon} \tag{10}$$

where, ν and CNU are the turbulent kinetic viscosity and the parameter, respectively.

In this model, the value of CNU was set to be 0.085.

4.3 Material properties and simulation conditions

Two different examples related to the situations described in this research were selected. Case I involves a water area and spillway length of an upstream reservoir that are larger than those of the downstream reservoir. Conversely, case II deals with an example in which the sizes of the downstream reservoir are greater compared to the upstream reservoir. These simulation conditions are shown in Table 3. The geometric relationships were modeled using AutoCAD software (version 2006, Autodesk, San Rafael, CA), and the three-dimensional solid geometries were simulated by the FLOW-3D software (version 10.1, Flow Science, Inc., Santa Fe, NM) in order to prove Equation (3). The ground of each reservoir matched the bottom levels of the spillways (to avoid the usage of unnecessary meshes). No-slip conditions on the boundaries were applied to minimize the effects of the properties of the ground and walls against the inflowing fluids. The slope of the intermediate channel connecting the upstream and downstream reservoirs was determined by calculating the ratio of the altitude difference to the actual length of the stream.

Table 3 Material properties and simulation conditions

	Variable		Value	Additional comments
	Fluid density		1000 kg/m^3	293.15 K (20°C)
	Fluid viscosity		0.001 Pa·s	Dynamic viscosity
	Gravity		9.8 m/s^2	
	Moving velocity of spillway		1.0 m/s	
Case I	Upstream reservoir (Daebaemi)	Water area of reservoir	3977.7 m^2	
		Length of spillway	1.3 m	
		Depth of spillway	2.0 m	
	Downstream reservoir (Darakmal)	Water area of reservoir	2904.6 m^2	
		Length of spillway	1.0 m	
		Depth of spillway	5.0 m	
	Width of intermediate channel		1.3 m	Width of upstream spillway
	Slope of intermediate channel		1.3%	Average value from geometry
Case II	Upstream reservoir (Anmal)	Water area of reservoir	4331.4 m^2	
		Length of spillway	5.8 m	
		Depth of spillway	1.0 m	
	Downstream reservoir (Naesuinpyeong)	Water area of reservoir	9821.8 m^2	
		Length of spillway	6.5 m	
		Depth of spillway	1.6 m	
	Width of intermediate channel		5.8 m	Width of upstream spillway
	Slope of intermediate channel		5.7%	Average value from geometry

A general moving object (GMO) is a rigid body in any type of physical motion that is coupled with a fluid flow. In order to break the spillway of the upstream reservoir, the GMO lifted the spillway up at a speed of 1.0 m/s. When the upstream spillway was in motion, the water exposed to the space that was newly opened from the bottom of the reservoir began to flow because of the stagnation pressure caused by gravity. Meshes of the complicated domain were divided into several parts to cut down on memory usage. Smaller meshes were used at

the inlet and outlet areas of the reservoirs and at the intermediate channels connecting the upstream and downstream reservoirs. To reduce the computational time, the total number of meshes and the different mesh sizes of each domain were empirically determined, as shown in Figure 3.

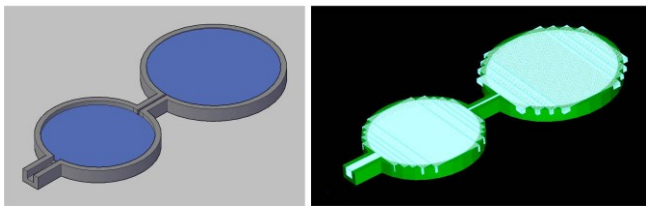

a. 3-D geometry b. Hexahedral meshes

Figure 3 3-D geometry and meshes in case I

A generalized minimum residual (GMRES) algorithm implemented in the software was activated to solve for the pressures and velocities[1,2,16]. A generalized conjugate gradient (GCG) algorithm was used to compute the viscous terms in the GMRES solver. It took about 10 days to accomplish each simulation using a personal computer (Intel® Xeon® CPU X5690@4.00 GHz (two processors), G.SKILL RAM 48GB@1,600 MHz). For case I, the fluid velocity distribution on the surfaces of the entire domain at time 150 s is shown in Figure 4.

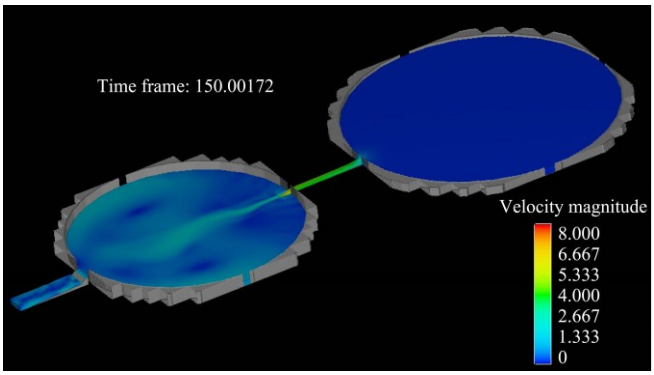

Figure 4 Fluid velocity distribution of the entire domain at 150 s in case I

5 Failure probability

The failure probability of the spillways was estimated based on the concept of structural safety. There is a structural similarity between retaining walls and spillways in that both structures resist lateral pressures. The structural safety of the spillway was also examined by assessing the levels of overturning, sliding, and settlement. The safety factor and limit state equations that are related to overturning are defined as follows:

$$F.S = \frac{\sum M_R}{\sum M_T} \tag{11}$$

$$g(x) = \sum M_R - \sum M_T \tag{12}$$

where, $F.S$ is the safety factor; ΣM_R is the summation of the resistant moment; ΣM_T is the summation of the overturning moment, and $g(x)$ is the limit state equation for overturning.

In addition, it is necessary to review spillway sliding because a spillway is a structure under active earth lateral pressures and hydraulic pressures. The earth pressures for the cases described herein were calculated by using Rankine's formula for active earth pressure. The safety factor and limit state equations can be calculated as follows:

$$F.S = \frac{\sum V tan\varphi}{\sum P} \tag{13}$$

$$g(x) = \sum V tan\varphi - \sum P \tag{14}$$

where, ΣP is the summation of active earth pressures and hydraulic pressures; ΣV is the summation of vertical pressures, and φ is the friction angle.

Because the elastic body of a spillway is on the ground as a plastic body, the settlement of spillways should be examined. The ultimate bearing capacity is the maximum pressure that the foundation soil is able to withstand without undergoing general, local, and/or punching shear failures due to the load. Therefore, the safety factor and limit state equations of the ultimate bearing capacity related to settlement are calculated as follows:

$$F.S = \frac{q_u}{q_{net}} = \frac{cN_cF_{cd}F_{ci} + qN_qF_{qd}F_{qi} + 0.5\gamma_t B'N_\gamma F_{\gamma d}F_{\gamma i}}{\frac{\sum V\left(1+\frac{6e}{B}\right)}{B}} \tag{15}$$

$$g(x) = \sum q_u - \sum q_{net} \tag{16}$$

where, q_u is the ultimate bearing capacity; q_{net} is the contact pressure; c is the cohesion of soil; q is the effective stress of the foundation (unit); γ_t is the unit weight of the foundation soil; B is the width of the foundation; B' is the effective width of the foundation; e is the eccentricity; N_c, N_q, and N_γ are the bearing capacity factors; F_{cd}, F_{qd}, and $F_{\gamma d}$ are the depth factors; and F_{ci}, F_{qi}, and $F_{\gamma d}$ are the load slope factors.

Safety factors related to spillway failure can be determined by the design criteria of the retaining wall under lateral pressure. The safety factors for overturning, sliding, and settlement of the retaining wall are generally required to be greater than 2.0, 1.5 and 3.0 times (by considering uncertainties of both soils and structures), respectively[3]. To calculate the failure probabilities of only downstream spillways, without considering the rise of water levels incurred by the collapse of upstream spillways, the full water level was assumed to be at the crest of the spillway, as shown in Figure 5a. The soil and hydraulic pressures described in Figure 5a were applied to the wall of the spillway, and the probability of each aspect of failure (including overturning, sliding, and settlement) was computed with Equations (12), (14) and (16), and Tables 2 and 3. To understand the effects of the collapse of an upstream spillway, the rise in the water level was reflected with the simple equation, as shown in Figure 5b.

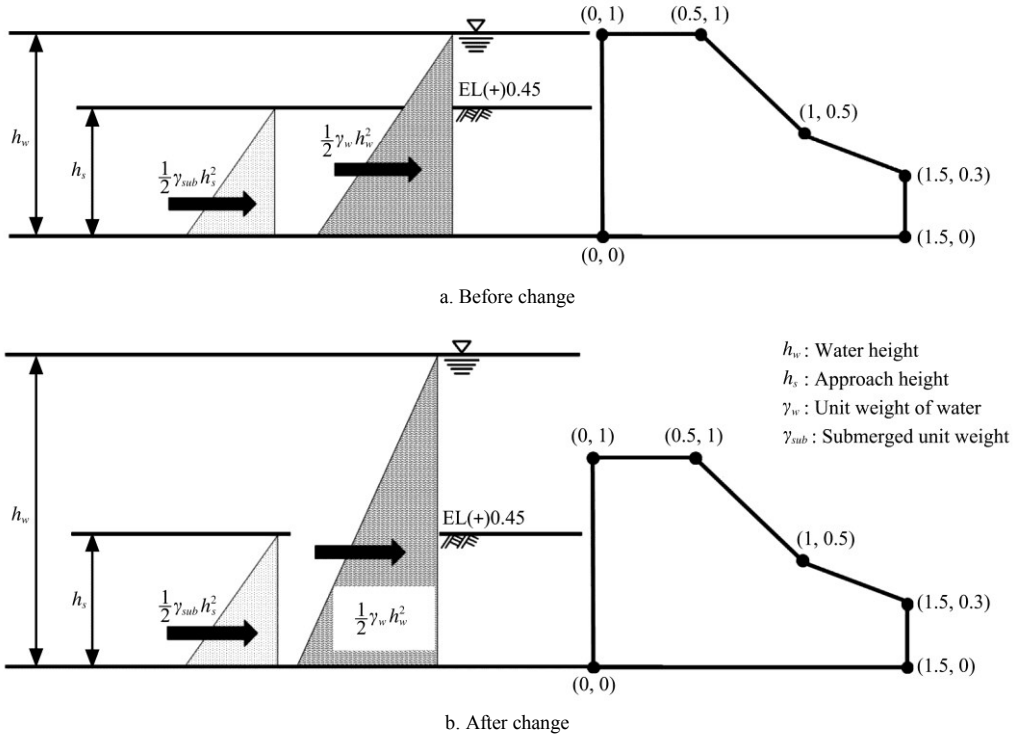

a. Before change

b. After change

Figure 5 Distributions of soil and hydraulic pressures before/after change of water level in the case of Darakmal reservoir

6 Results and discussion

6.1 The rise of the water level

Fluctuated waves on the surface of the downstream reservoir in case I were not observed, as shown in Figure 6. In case II, however, fluctuated waves periodically occurred during the overall flowing time because the average slope of the intermediate channel was more than four times the average slope of the intermediate channel in case I (Table 3). Due to the fact that the length ratio of the upstream spillway to the downstream spillway, the potential capacity (water volume) surrounded by the depth of the upstream spillway, and the water area of the upstream reservoir in case I were all larger than the corresponding values in case II, the rise of the water level in the downstream spillway in case I was larger than it was in case II. The increased water levels in the spillways of downstream reservoirs are shown in Table 4.

Table 4 Increases in the water levels in the spillways of the downstream reservoirs

Case	Method	Rise of water level/m	Relative error/%
Case I	Simple equation	1.005	+ 0.17
	Simulated result	1.003	
Case II	Simple equation	0.534	+ 4.92
	Simulated result	0.509	

Given the fact that our proposed simple equation is based upon the assumption that the velocity of the stream inflowing into the downstream reservoir from the

upstream reservoir is zero, a relatively small error was observed in case I. In case II, the maximum values of the water level (excluding the kinetic energies at the spillway of the downstream reservoir) were 0.509 and 0.570 m at times of 42 and 262 s, respectively. However, the influence on the response range of the time zone with a water level of 0.509 m was longer than it was for a water level of 0.570 m. Therefore, in a practical sense, a water level of 0.509 m can be used to facilitate the optimal design of the spillway.

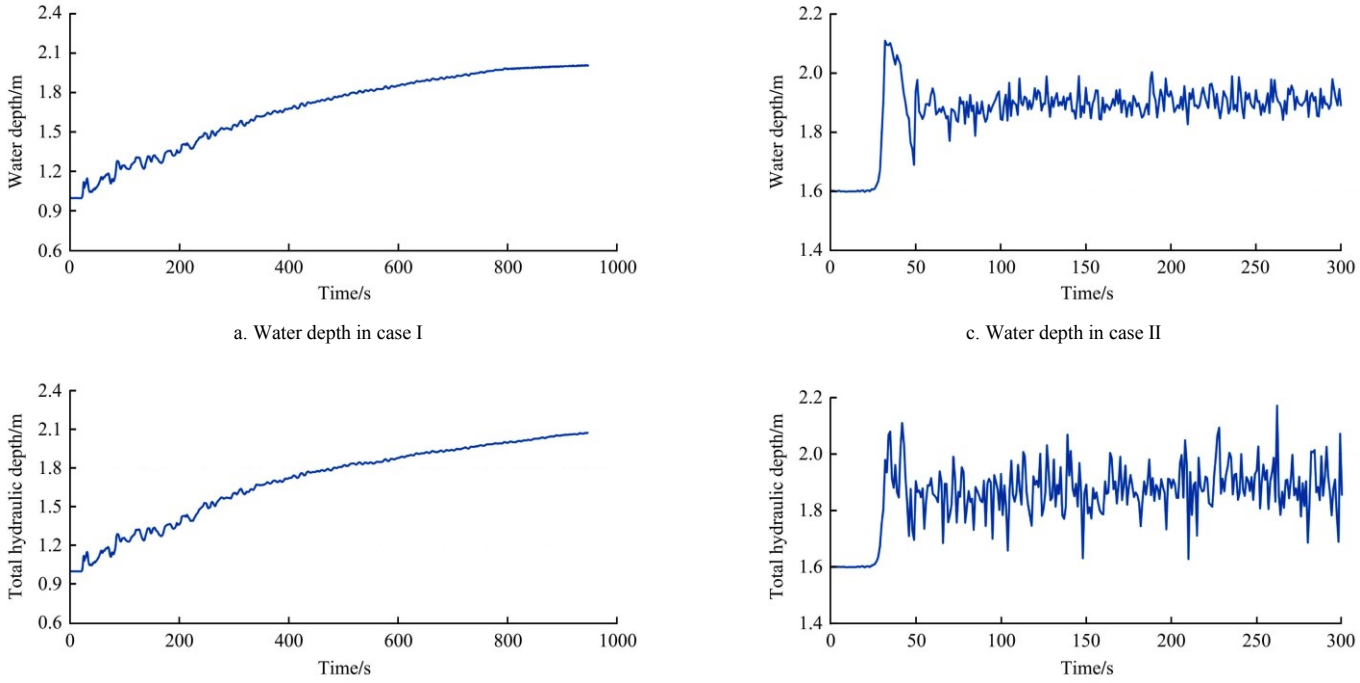

a. Water depth in case I

b. Total hydraulic depth in case I

c. Water depth in case II

d. Total hydraulic depth in case II

Figure 6 Energy depths at the spillways of the downstream reservoirs

6.2 Failure probability

6.2.1 Safety factor

Safety factors for overturning, sliding, and settlement were calculated by using the averaged values (excluding the coefficients of variations), as shown in Table 5. When assessed using the single mode in case I, the individual safety factors were over the safety margin. However, when assessed in sequential mode, the safety factors were under the safety margin. The greatest changes in the values were clearly observed for the settlement. In reality, flooding from upstream reservoirs can affect the flow conditions of downstream. However, because we assumed the worst-case scenario, where all of the water in the upstream reservoir flowed into the downstream reservoir without any water loses, water overflow and the downstream traveling time were not considered. Therefore, the safety factor of the lower spillway may be a little higher than the calculated value.

Table 5 Safety factors of downstream spillways in cases I and II

Reservoir		Safety factor		
		Single mode	Sequential mode	Increase/%
Darakmal (case I)	Overturning	9.04	1.16	1.28E+02
	Sliding	12.20	3.20	2.62E+02
	Settlement	9.13	3.00	3.29E+02
Naesuinpyeong (case II)	Overturning	11.40	5.28	4.63E+01
	Sliding	8.54	5.22	6.11E+01
	Settlement	7.12	4.68	6.57E+01

Table 6 Failure probability of downstream spillways in cases I and II

Reservoir		Failure probability		
		Single mode	Sequential mode	Increase/%
Darakmal (case I)	Overturning	0	2.640E-01	∞
	Sliding	4.24E-04	2.477E-01	5.84E+02
	Settlement	1.08E-03	2.803E-01	2.60E+02
Naesuinpyeong (case II)	Overturning	2.63E-21	6.794E-04	2.58E+19
	Sliding	3.90E-05	1.107E-01	2.84E+03
	Settlement	1.07E-05	1.166E-02	1.09E+02

6.2.2 Failure probability

The overturning, sliding, and settlement failure probabilities of downstream spillways increased since the collapse of upstream spillways. In particular, the failure probabilities related to overturning were exponentially increased. The failure probabilities due to sliding were the next highest. In South Korea, many reservoirs are connected to each other in series, and the distances between reservoirs are relatively short in comparison to serial reservoir systems in other countries[14]. This proximity among the reservoirs is due to the unique geographic characteristics of South Korea. To make matters worse, many reservoirs are over 60 years old. The management of these reservoirs has been neglected since their initial construction. Because the goal of spillways is to control floods, rising water levels can be dangerous in situations where upstream spillways in serial reservoirs collapse.

7 Conclusion

The proposed simple method for calculating the rise of water levels in the spillways of lower reaches caused by the collapse of upstream spillways in serial reservoirs was derived based on the discharge equation of overflowing weirs and the scaling law for continuous flow. The values predicted through our simple formula were close to the data simulated by FLOW-3D (within a maximum relative error of 5%). The rises in water levels of the downstream spillways were updated to recalculate the effects of water pressure loads on the walls of downstream spillways. The failure probabilities of the downstream spillways, in terms of sliding, overturning, and settlement failures, were computed with these values. This study found that the failure probabilities for independent components of reservoirs are significantly different from the systematic failure that results from the sequential flow of water through a serial system. The largest increases of the failure probabilities for downstream spillways were observed in overturning. The main governing factor for the collapse of spillway can be changed depending on the calculation method (i.e., the safety factor or failure probability). In the future, our proposed simple equation can be used to compute the failure probabilities of agricultural structures located in series or in parallel systems. Its applications will be further extended to understand the system dynamics of agricultural components in real-time.

Acknowledgment

The work was supported by a research grant of Chungbuk National University in 2012.

[References]

[1] Ashby S F, Manteuffel T A, Saylor P E. A taxonomy for conjugate gradient methods. SIAM J. Numer. Anal., 1990; 27: 1542–1568. doi: http://dx.doi.org/10.1137/0727091

[2] Barrett R, Berry M, Chan T F. Templates for the Solution of Linear Systems: Building Blocks for Iterative Methods, Philadelphia: SIAM. 1994. doi: http://dx.doi.org/10.1137/1.9781611971538

[3] Braja M D. Principles of foundation engineering, Toronto, Canada: Thomson, 1970; 390–393 p.

[4] Burcharth H F, Sorensen J S, Christiani E. On the evaluation of failure probability of monolithic vertical wall breakwaters. Proc. International Workshop on Wave Barriers in Deepwaters, 10-14 January, Yokosuka, Japan, 1994; 458–469.

[5] Chanel P G, Doering J C. Assessment of spillway modeling using computational fluid dynamics. Can. J. Civil Eng., 2008; 35(12): 1481–1485. doi:http://dx.doi.org/10.1139/L08-094

[6] Christiani E, Burcharth H F, Sorensen J D. Reliability based optimal design of vertical breakwaters modelled as a series system failure. Proc. the twenty-fifth international conf., 2-6 September, Orlando, FL, USA, 1996; 1589–1602.

[7] Hirt C W, Nichols B D. Volume of fluid (VOF) method for the dynamics of free boundaries. J. Comput. Phys., 1981; 39(1): 201–225. doi:http://dx.doi.org/10.1016/0021-9991(81)90145-5

[8] Hirt C W, Sicilian J M. A porosity technique for the definition of obstacles in rectangular cell meshes. Proc., 4th Int. Conf. on Numerical Ship Hydrodynamics, National Academy of Science Conf., 24-27 September, Washington, DC, USA, 1985; 1–19.

[9] Hirt C W. Volume-fraction techniques: powerful tools for wind engineering. J. Wind Eng. Ind. Aerodyn., 1993; 46/47: 327–338. doi: http://dx.doi.org/10.1016/0167-6105(93)90298-3

[10] Johnson M C, Savage B M. Physical and Numerical Comparison of Flow over Ogee Spillway in the Presence of Tailwater. J. Hydraulic Eng., 2006; 132(12): 1353–1357.

doi: http://dx.doi.org/10.1061/(ASCE)0733-9429(2006)132:12(1353).

[11] Kocaman S, Hatice O-C. The effect of lateral channel contraction on dam break flows: Laboratory experiment. J. Hydrol., 2012; 432/433: 145–153. doi: http://dx.doi.org/10.1016/j.jhydrol.2012.02.035

[12] Korea Rural Community Corporation. Emergency action plan (EAP) report. KRC, South Korea, 2008-2010.

[13] Korea Rural Community Corporation. Precision safety inspection (PSI) report. KRC, South Korea, 2006-2010.

[14] Ministry for Food, Agriculture, Forestry and Fisheries. Development of integrated management system for agricultural infrastructure report. MIFAFF, South Korea, 2014.

[15] Nichols B D, Hirt C W, Hotchkiss R S. Volume of fluid (VOF) method for the dynamics of free boundaries. Los Alamos Scientific Lab. Rep., LA-8355, Los Alamos, NM, USA. 1980.

[16] Saad Y, Schultz M H. GMRES: A generalized minimal residual algorithm for solving nonsymmetric linear systems. SIAM J. Sci. Stat. Comput., 1986; 7(3): 856–869. doi: http://dx.doi.org/10.1137/0907058

[17] Savage B M, Johnson M C. Flow over ogee spillway: physical and numerical model case study. J. Hydraulic Eng., 2001; 127(8): 640–649. doi: http://dx.doi.org/10.1061/(ASCE)0733-9429(2001)127:8(640).

[18] Vasquez J A, Roncal J J. Testing River2D and Flow-3D for sudden dam-break flow simulations. Proc., CDA 2009 Annual Conf., 3-8 October, Whistler, BC, Canada, 2009; 44–55.

[19] Versteeg H K, Malalasekera W. An introduction to computational fluid dynamics, New York: Longman Scientific and Technical. 1995.

[20] Xu Y, Zhang L, Jia J. Lessons from catastrophic dam failures in August 1975 in Zhumadian, China. GeoCongress 2008 (2008 proc., ASCE), 9-12 March, New Orleans, LA, USA, 2008; 162–169. doi: http://dx.doi.org/10.1061/40971(310)20.